Ecological Modelling 464 (2022) 109840

Contents lists available at ScienceDirect

Ecological Modelling

journal homepage: www.elsevier.com/locate/ecolmodel

Linking a compartment model for West Nile virus with a flight simulator for vector mosquitoes

Antje Kerkow [a,b,c,*], Ralf Wieland [a], Jörn M. Gethmann [d], Franz Hölker [b,c], Hartmut H.K. Lentz [d]

[a] Leibniz Centre for Agricultural Landscape Research (ZALF), Eberswalder Str. 84, 15374 Müncheberg, Germany
[b] Leibniz-Institute of Freshwater Ecology and Inland Fisheries (IGB), Müggelseedamm 310, 12587 Berlin, Germany
[c] Freie Universität Berlin, Department of Biology, Chemistry, Pharmacy, Institute of Biology, Königin-Luise-Str. 1-3, 14195 Berlin, Germany
[d] Friedrich-Loeffler-Institut (FLI), Institute of Epidemiology, Südufer 10, 17493 Greifswald - Insel Riems, Germany

ARTICLE INFO

Keywords:
Agent-based models
Aedes japonicus japonicus
Germany
Pica pica
SEIR/SIR models
Spatial component

ABSTRACT

Compartmental SIR and SEIR models have become the state of the art tools to study infection cycles of arthropod-borne viruses such as West Nile virus in specific areas. In 2018, the virus was detected for the first time in Germany, and incidents have been reported in humans, birds, and horses.

The aim of the work presented here was to provide a tool for estimating West Nile virus infection scenarios, local hotspots and dispersal routes following its introduction into new locations through the movements of mosquitoes. For this purpose, we adapted a SEIR model for West Nile virus to the conditions in Germany (temperatures, geographical latitude, bird and mosquito species densities) and the characteristic transmission and life trait parameter of a possible host bird and vector mosquito species. We further extended it by a spatial component: an agent-based flight simulator for vector mosquitoes. It demonstrates how the female mosquitoes move within the landscape due to habitat structures and wind conditions and about how many of them leave the region in the different cardinal directions.

We applied the space–time coupled model with a daily temporal and spatial resolution of 100 m × 100 m to the Eurasian magpie (*Pica pica*) and the Asian bush mosquito (*Aedes japonicus japonicus*). Both species are widely distributed in Germany and discussed as important hosts and vectors, respectively. We also applied the model to three study regions in Germany, each representing slightly different climatic conditions and containing significantly different pattern of suitable habitats for the mosquito species.

1. Introduction

1.1. Background

West Nile virus (WNV) is an arthropod borne pathogen maintained in enzootic transmission cycles between birds (amplifying hosts) and ornithophilic mosquitoes (vectors) (Chancey et al., 2015; Marini et al., 2018). Humans, horses and other mammals may be dead-end hosts. In 2018, Europe experienced an intense and long heat wave, bringing the continent its worst WNV epizootics and epidemics to date. Germany was affected for the first time with 12 confirmed infections in birds and 2 in horses (Ziegler et al., 2019; Kampen et al., 2020; Ziegler et al., 2020). In the following years, repeated cases occurred in the affected regions in Germany and beyond, indicating that the virus hibernates in local mosquito populations (Kampen et al., 2020; Ziegler et al., 2020; Neupert, 2020; Pietsch et al., 2020).

Many bird species seem susceptible to the virus (Linke et al., 2007), but only some develop high viraemiae and death rates (Jourdain et al., 2007; Pérez-Ramírez et al., 2014). Especially birds of prey and corvids were observed to have high mortality from WNV-2 in Europe. Severely affected species include Northern goshawk (*Accipiter gentilis*), house sparrow (*Passer domesticus*), Eurasian magpie (*Pica pica*) and hooded crow (*Corvus cornix*) (Calistri et al., 2010; Zehender et al., 2017; Bażanów et al., 2018; la Puente et al., 2018; Hubálek et al., 2018, 2019; Napp et al., 2019). Based on field studies in Spain, Napp et al. (2019) propose the Eurasian magpie as a sentinel species. It is one of the most common corvid species in Europe, sedentary and showed high virus susceptibility, virus titres and mortality in experimental studies (de Oya et al., 2018).

The main vectors of WNV in Europe are supposed to be mosquitoes of the widespread *Cx. pipiens* complex including the two biotypes *Cx. p. pipiens* and *Cx. p. molestus*, as well as *Cx. torrentium* and *Cx. modestus* (Leggewie et al., 2016; Tran et al., 2017; Bhowmick et al., 2020; Holicki et al., 2020). Besides those, *Ae. vexans* and *Ae. japonicus*

* Corresponding author at: Leibniz-Institute of Freshwater Ecology and Inland Fisheries (IGB), Müggelseedamm 310, 12587 Berlin, Germany.
E-mail address: antje.kerkow@igb-berlin.de (A. Kerkow).

https://doi.org/10.1016/j.ecolmodel.2021.109840
Received 12 March 2021; Received in revised form 31 October 2021; Accepted 16 November 2021
Available online 9 December 2021

japonicus are also considered species (Kampen et al., 2020). Especially the potential future role of the invasive Asian bush mosquito *Ae. j. japonicus* is currently hotly debated (Schaffner et al., 2009; Kampen et al., 2020). Laboratory experiments with specimens collected in Switzerland and the US revealed a significantly shorter virus incubation period (Turell et al., 2001) and significantly higher dissemination and transmission rates than *Cx. pipiens sl.* (Veronesi et al., 2018; Wagner et al., 2018; Turell et al., 2001; Sardelis and Turell, 2001), but another laboratory study with individuals caught in Germany showed a resistance to infections with West Nile virus (Huber et al., 2014). *Aedes j. japonicus* was detected in Germany in 2008 (Koban et al., 2019) and is mainly established in the western and southern part of the country (Kampen et al., 2020).

Because of the medical relevance of the virus it is highly important to take precautionary measures in the potential risk areas. Models shall help to understand the complex interrelationships that contribute to the establishment of an epizootic, identify high-risk areas, and assess the effect of precautionary measures. So far, WNV models focused either on the spatial or the systemic component. The spatial models identify potential risk areas by modelling the habitats of vector mosquitoes (Cooke et al., 2006; Diuk-Wasser et al., 2006; Pape et al., 2008), host birds (Durand et al., 2017) or an overlap of both (Tran et al., 2017). Other spatial approaches aim to identify WNV risk areas by analysing the climate and other spatial features of areas where epizootics have occurred (Brownstein et al., 2002; Harrigan et al., 2014; Tran et al., 2014).

Compartment models based on differential equations are much more complex and focus on the systemic component. They consider both seasonal and temperature-dependent population densities of host birds and vector mosquitoes and simulate the development of the infection processes after virus introduction in a given region. Since about 20 years these models have been successfully used to study arbovirus infection cycles like that of WNV (Thomas and Urena, 2001; Wonham et al., 2004; Laperriere et al., 2011; Simpson et al., 2012). The models are called SIR or SEIR models, which refers to the infection stages in which the model organisms can be found: “Susceptible”, (“Exposed”), “Infected–infectious” and, only valid for the vertebrate hosts, “Recovered and Immune”. They assume a homogeneous distribution of host birds and vector mosquitoes in a given outbreak region and are usually calibrated by means of the number of encountered dead birds (Rubel et al., 2008; Laperriere et al., 2011).

Due to the assumption of homogeneity in previous compartmental WNV models, it was not possible to locate the risk areas more precisely, to investigate influences of regionally different contact rates between hosts and vectors, and to estimate simultaneously the spread of the virus within the region and beyond. To achieve this, one needs a spatial component that considers the locations and movements of the animals. In the work presented here, we will extend a compartment model for WNV by a spatial component: a flight simulator and localiser for vector mosquitoes. We focus on the local occurrence and movements of vector mosquitoes to estimate the virus spread because it can be effectively controlled by decimating mosquito populations. On the wild bird side, no vaccination exists so far and population control would be difficult to establish and not be a socially accepted measure. Furthermore, the active (autonomous) movements of mosquitoes are usually of smaller distance and more predictable than those of the vector birds.

We further discovered that in existing compartmental WNV models (Wonham et al., 2004; Laperriere et al., 2011) the calculation of an unknown parameter in the infection equations, the vector population size in the epidemic area, is problematic. This is because the contact rate of vector mosquitoes with host birds has a huge impact on the equations in these models, but is solely derived from observations of temperature-dependent blood digestion. The linkage between the duration of blood digestion and frequency of host contacts is plausible. However, it was numerically not considered that the vector mosquitoes integrated in the model (an aggregation of *Culex pipiens sl.* and other *Culex* species, especially *Cx. tarsalis*) do not feed exclusively on the host birds with every required blood meal. Other birds as well as mammals, amphibians and reptilians are, for example, also used by both biotypes of *Cx. pipiens* (Apperson et al., 2004). As a result of this set-up, the population density of the vector mosquitoes was calculated to be significantly too low, in our opinion. Conversely, if the model is applied to new epidemic areas with only a few case numbers and if mosquito densities confirmed by monitoring campaigns are integrated, the model will considerably overestimate the course of infection due to the high contact numbers. The problem becomes even more apparent when the model is applied to the mosquito species *Ae. j. japonicus*, which is mammophilic and therefore seeks out humans and mammals more frequently than birds for its blood meal (Molaei et al., 2009; Schönenberger et al., 2016). The model thus needs a factor for the proportion of mosquito blood meals taken on the host birds.

1.2. Objectives

We aimed to provide a model that, after introduction of the virus into a new area, can (i) predict the potential regional extent of an epizootic based on realistic density data of host birds and amplifying vector mosquitoes, (ii) identify high-risk transmission hotspots within the region, and (iii) estimate the local spread of the virus into surrounding areas by mosquito emigration. The latter two model features are intended to support targeted mosquito control measures to contain the virus. Furthermore, we are investigating the effects of consistent population losses on the mosquito side due to unfavourable regional landscape patterns on infection chains.

1.3. Model implementation and applications

We numerically adapted an existing model for WNV implemented for Minneapolis in the US (Laperriere et al., 2011) and extended it by a spatial component, an agent based flight simulator for vector mosquitoes. Agent-based models (ABMs) have successfully been used for the dispersion modelling of insects and other mosquitoes (Knighton et al., 2014; Parry et al., 2006; Manore et al., 2015). The advantage of this type of model is that it can represent environmentally induced behaviour changes, random decisions, interactions between individuals (the agents) and agent heterogeneity (de Almeida et al., 2010).

The space–time coupled model is applied to 3 study regions in Germany with a size of 625 km^2 each, but a considerably different number and distribution of vector mosquito habitats and slightly different climatic conditions. The host birds in the model are represented by the Eurasian magpie (*P. pica*), and the vector mosquitoes by the Asian bush mosquito (*Ae. j. japonicus*). The latter was used for the development of the spatial component because a well validated, model-based habitat map for the species in Germany already exists (Kerkow et al., 2019). Due to its high resolution, it is a suitable basis for flight simulations and local density estimates. The magpie, on the other hand, was integrated into the model not only because of its host characteristics described in Section 1.1, but also because the species occurs in urban habitats, especially in parks, cemeteries, allotment gardens, as well as in semi-open and open landscapes (Geodon et al., 2014). Therefore, its habitat may overlap with that of *Ae. j. japonicus* to a large extent (Kerkow et al., 2019), principally allowing for frequent contacts with the mosquito species.

1.4. Summary of model innovations

Our work presents the following innovations to existing WNV models:

(i) a numerical adaptation that considers mosquito blood meals on organisms other than the host birds. This is useful for the integration of real density data of vector mosquitoes and thus enables the model to be applied to regions where the virus has not yet circulated for a long time and where case numbers are still low.
(ii) the extension by a spatial component, an agent-based flight simulator for vector mosquitoes which illustrates the possible regional distribution and, taking into account the habitat structure, simulates the self-motion of the mosquitoes and estimates how many of them would probably leave the region towards which cardinal points.
(iii) an adjustment in the calculation of infection trajectories by estimated habitat-related persistent population losses on the mosquito side.

2. Materials and methods

2.1. Overview

The model has two components that interact with each other. These are, on the one hand, a temporal component, an adaptation of the SEIR model of Laperriere et al. (2011), that describes the population dynamics of host birds and vector mosquitoes by means of temperature- and seasonal-dependent ordinary differential equations and calculates the proportions of the mosquito and bird specimens in their respective infection stages. On the other hand, there is a spatial component that describes local occurrences and movements of vector mosquitoes and estimates the impact of different landscape structures on populations as well as the daily emigration rate from a possible epidemic area towards the different cardinal points. By manipulating the mosquito population, the spatial component intervenes in the differential equations of the temporal component. The composite model has a daily time resolution and a spatial resolution of 100 m × 100 m.

Entities in the model are Eurasian magpies (*Pica pica*), female mosquito imagoes and female mosquitoes in pre-imaginal, aquatic stages (males have no blood meals and thus do not contribute to the trans-sylvatic transmission cycle). The mosquitoes belong to the species *Aedes japonicus japonicus* (Asian bush mosquito). For the sake of simplicity, we call the imagoes "mosquitoes" and the mosquitoes in the preimaginal stages "larvae" as it is done in Laperriere et al. (2011).

The spatial component is based on a two-dimensional habitat suitability map for *Ae. j. japonicus*. The map has been developed using a nested modelling approach consisting of (i) a part that models the global, climatic requirements (Wieland et al., 2017; Früh et al., 2018; Kerkow et al., 2020) and (ii) a separate part that integrates local land use requirements and the influence of wind speed (Kerkow et al., 2019). It covers the area of Germany, has a resolution of 100 m × 100 m and shows the habitat suitability as values between 0 and 1. The grid map can be freely downloaded under the link "https://doi.org/10.4228/zalf.dk.90". Due to its high score in evaluation as measured by the hit rate of data that were not included in a model training, we assume that it correlates with the larval density in areas where the invasive species is already established and widely distributed since several years.

Process overview and scheduling. A main simulation calls both, the temporal component (SEIR model) and the spatial component (flight simulator), and synchronises the mosquito population size and the number of infectious mosquitoes. At each time step, first the numbers of mosquitoes and birds in their respective infection stage is changed by the daily hatching and mortality rates implemented in the temporal component. The temporal component uses the information stored by the main model for the previous day for the calculations. The numbers of infectious and non-infectious mosquitoes are then communicated to the spatial component which may reduce it by simulated deaths due to large energy consumption (e.g. after long flights or long stays in unsuitable landscapes). The reduced number is then transmitted to the main component. At the beginning of the simulation, the temporal component uses initialisation parameters.

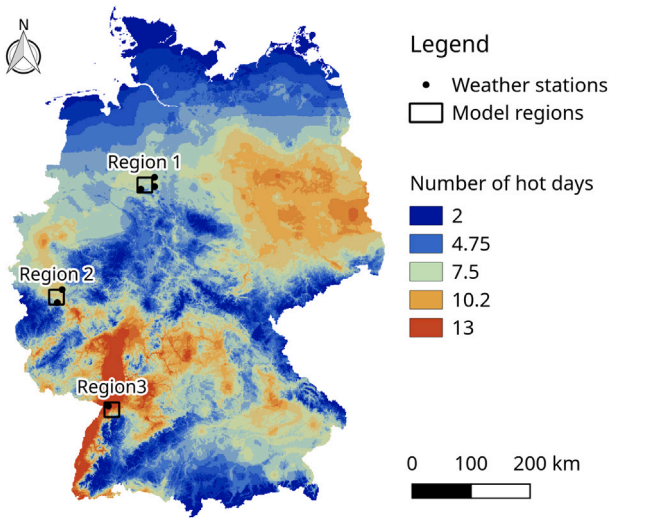

Fig. 1. Location of the study regions, their nearest weather stations, and, as a risk indicator for epizootics, illustration of the number of local hot days defined by a maximum air temperature higher than 30°C (annual mean of the long-term period 1981–2010). Geodata source: German Weather Service.

2.2. Study regions

We selected three regions within the grid based habitat suitability map with sizes of 625 km² (25 km × 25 km) for model applications (Figs. 1 and 2). In each of them, the occurrence of *Ae. j. japonicus* has been documented for several years (Werner and Kampen, 2013; Kampen et al., 2016; Walther and Kampen, 2017; Kampen et al., 2017; Koban et al., 2019). In areas that include our study regions 2 and 3, the species has spread rapidly and the larval numbers on the sampling sites have increased dramatically since the first evidence. Region 1 appeared to have a lower spreading potential and larval numbers at the collection sites were partially declining.

The regions differ in their climatic conditions. The average annual temperature and the number of hot days (average temperature above 30°C) increases from north to south (Fig. 1). The occurrence of a high number of hot days is an important risk indicator for the occurrence of mosquito-borne diseases (Brugger and Rubel, 2009; Filippelli et al., 2020). Furthermore, the regions differ in their average habitat suitability for *Ae. j. japonicus* as calculated by Kerkow et al. (2019). It is 0.35 in region 1, 0.66 in region 2 and 0.79 in region 3 (Fig. 2).

2.3. Temporal component

2.3.1. Compartments

The model is based on 9 compartments (ordinary differential equations) that describe the populations and infection stages of mosquitoes and birds by means of a density-dependent approach. An overview of the SEIR model including the influence of the flight simulator is given in Fig. 3.

The mosquito compartments include larvae (L_M), virus susceptible (S_M), exposed (E_M) and infectious mosquitoes (I_M). The mosquitoes develop from the larvae, whose number is initially determined by the average estimated habitat suitability of the region (see Section 2.3.3). Both, larvae and mosquitoes have general temperature-dependent mortality rates but cannot succumb to infection. The number of susceptible and infectious mosquitoes is also corrected by losses (x_{S_M}, x_{I_M}) communicated by the flight simulator.

The bird compartments are susceptible (S_B), exposed (E_B), infectious (I_B), recovered (R_B) and dead birds (R_B). Chicks are always virus succeptible after hatching. Recovered birds have always acquired immunity and the dead birds refer only to those that have succumbed

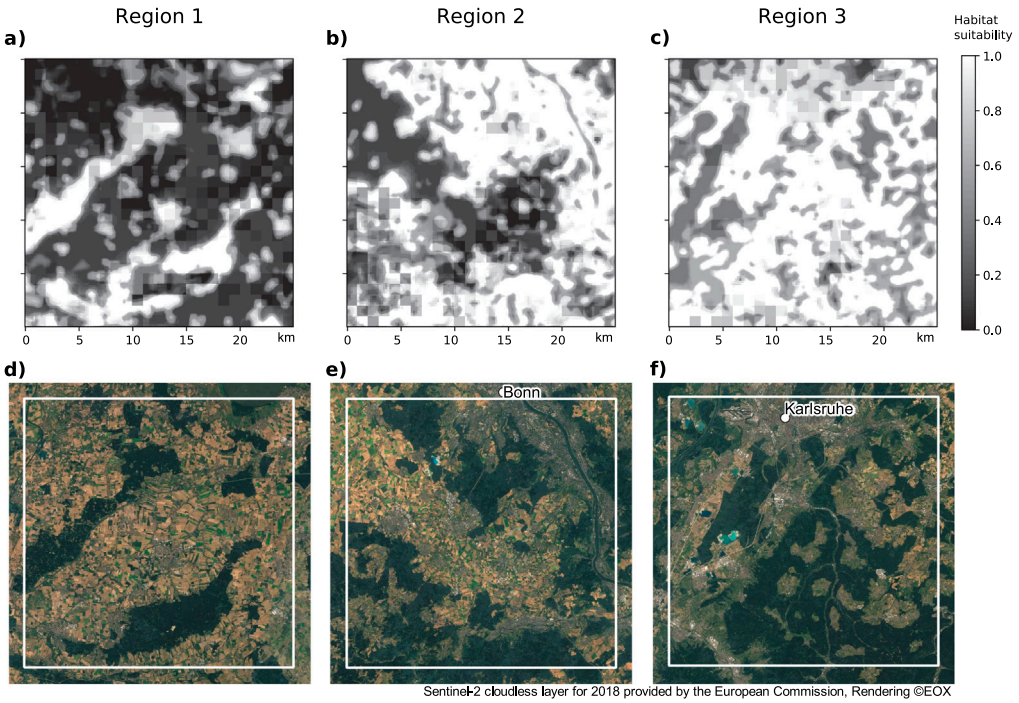

Fig. 2. Top (a,b,c): Study regions and their habitat qualities for *Aedes japonicus japonicus* on a scale from 0 (poor quality) to 1 (high quality). The habitat map was created using a separately published model (Kerkow et al., 2019) and includes climatic and landscape features as well as regional mean wind speeds. Particularly good habitats are less exposed to wind and belong, for example, to green urban areas, cemeteries, gardens, zoos or deciduous forests. Bottom (d,e,f): Satellite images of the study regions visualising the landscapes.

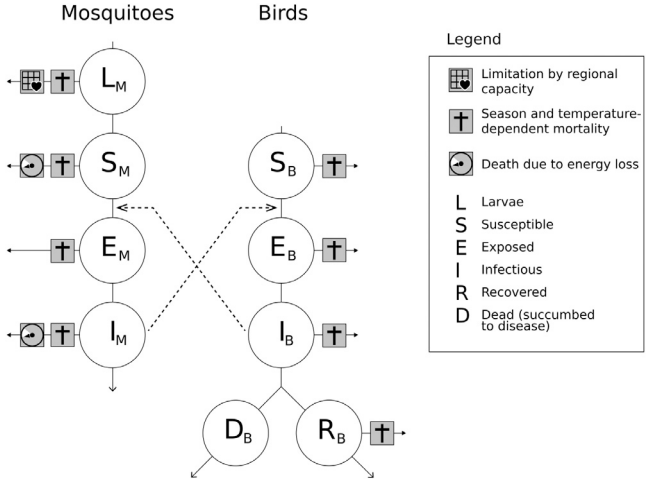

Fig. 3. Possible chain of infection stages that vector mosquitoes and host birds in the model may undergo; The crosses symbolise the mortalities to which the animals are subject at each stage of infection depending on season and temperature. The dashed arrows symbolise the virus exposure of mosquitoes and birds after contact with an infectious animal of the other species. On the mosquito side, the influence of the spatial model extension (the flight simulator) becomes visible by the determination of the number of larvae and the energy-related mosquito mortality.

to WNV. Like the mosquitoes, all birds have a general temperature-dependent mortality rate. Infection occurs upon mixing a fraction of infectious and susceptible mosquitoes or birds, respectively. Vertical virus transmission from mosquito females to offspring as well as horizontal transmission between birds is neglected.

The compartment equations (Eq. (1)–(9)) are taken from previous compartment models for Usutu virus and WNV (Rubel et al., 2008; Laperriere et al., 2011), but we introduced a species specific probability of the mosquitoes taking blood meals on a bird and an additional probability of taking blood meals on a host bird when feeding on a bird. Both factors affect the virus transmission rates (see Eqs. (10), (11)).

Mosquitoes:

$$\frac{dL_M}{dt} = (b_L(T)\delta_M(D)N_M - m_M(T)L_M)\left(1 - \frac{L_M}{K_M}\right) - b_M(T)L_M \quad (1)$$

$$\frac{dS_M}{dt} = (b_M(T)L_M - m_M(T)S_M - \lambda_{BM}(T,D)S_M) - x_{S_M} \quad (2)$$

$$\frac{dE_M}{dt} = \lambda_{BM}(T,D)S_M - \gamma M(T)E_M - m_M(T)E_M \quad (3)$$

$$\frac{dI_M}{dt} = (\gamma M(T)E_M - m_M(T)I_M) - x_{I_M} \quad (4)$$

Birds:

$$\frac{dS_B}{dt} = \left(b_B - (b_B - m_B)\frac{N_B}{K_B}\right)N_B - \lambda_{MB}(T,D)S_B - m_B S_B \quad (5)$$

$$\frac{dE_B}{dt} = \lambda_{MB}(T,D)S_B - \gamma_B E_B - m_B E_B \quad (6)$$

$$\frac{dI_B}{dt} = \gamma_B E_B - \alpha_B I_B - m_B I_B \quad (7)$$

$$\frac{dR_B}{dt} = (1-\nu_B)\alpha_B I_B - m_B R_B \quad (8)$$

$$\frac{dD_B}{dt} = \nu_B \alpha_B I_B \quad (9)$$

The number of susceptible mosquitoes exposed on a simulation day (λ_{BM}) depends on the proportion of active mosquitoes (δ_M), the transmission rate from infectious bird to susceptible mosquito (β_B, see Table 3), and the average ratio of infectious birds to all *P. pica* host birds (I_B/K_B) (Eq. (10)). The number of exposed birds (λ_{MB}) depends on the fraction of active mosquitoes, the transmission rate from infectious mosquito to susceptible bird (β_M, see Table 3), and the average ratio of infectious mosquitoes to *P. pica* host birds (I_M/K_B) (Eq. (11)).

$$\lambda_{BM}(D,T) = \delta_M(D)\beta_B(T)\frac{I_B}{K_B} \quad (10)$$

$$\lambda_{MB}(D,T) = \delta_M(D)\beta_M(T)\frac{I_M}{K_B} \quad (11)$$

The differential equations were solved with the Euler method (a comparative test for the solution of the decoupled SEIR model with the Runge–Kutta(4) method showed only a marginal deviation compared to the calculation with the Euler method – uncertainties in the parameter estimation have a greater influence on the calculated infections). To trigger West Nile virus infections in the study regions during a model application, we introduce infectious birds into the system 3 times a year: 2 at the beginning of March (after the arrival of migratory birds), 2 at the end of July (end of the main chick hatching period) and 4 at the beginning of October, as some WNV vector bird species migrate intercontinental in autumn.

2.3.2. Temperature and day length

The temporal component is driven by means of daily average temperature data and the day length. Temperature data was obtained from the German Weather Service. We chose one to three weather stations close to every study region (Fig. 1) and, if they were several, calculated the average temperature. The temperature values are smoothed with a weighted average filter and a window size of 2 (Fig. AF1 in the appendix).

For the calculation of the day lengths (Fig. AF2 in the appendix), we apply the Brock model (Brock, 1981; Forsythe et al., 1995) which maps the latitude of the location and the day of the year on the day length (equation AE2 in the appendix). Our study regions are located at latitudes 48.9, 50.6 and 52.4. We run all model applications by the average day length of the regions of 50.6. Tests showed that the slightly different latitudes of the regions do not lead to any difference in the model results regarding the number of infected birds and mosquitoes.

2.3.3. Initialisation

The initial conditions and initialisation parameters of the temporal component are listed in Table 1. Our model applications start on January 1st and we assume that no infection has yet been introduced into the region, hence all mosquitoes and birds are assigned as virus succeptible. As in the model applications of Laperriere et al. (2011), the bird population is set to the maximum as defined by the carrying capacity of the region, and the minimum number of mosquitoes required to prevent extinction is 15% of the carrying capacity of the larvae. The estimation of the respective regional carrying capacities for mosquito larvae is given below, for birds it is explained in the appendix. Note that the carrying capacity of the bird population makes it appear that the number can be determined that accurately, but this is not the case. At an early stage of modelling, we tried to estimate the number precisely because the original SEIR model was unreasonably sensitive to that parameter. By integrating the blood meal rate on vector birds, we made the model no longer sensitive to small changes in bird numbers.

Table 1
Initial conditions and initialisation parameters.

Term	Value	Description
K_B	8,226	Carrying capacity of host birds (magpies)
$K_{M_{max}}$	19,900,000	Carrying capacity of mosquito larvae in a perfect habitat
$K_{M_{R1}}$	6,965,000	Carrying capacity of mosquito larvae in Region 1
$K_{M_{R2}}$	13,134,000	Carrying capacity of mosquito larvae in Region 2
$K_{M_{R3}}$	15,721,000	Carrying capacity of mosquito larvae in a Region 3
$N_{M_{min}}$	$K_M \times 0.15$	Minimum number of mosquitoes
S_B	K_B	Amount of susceptible birds
E_B	0	Amount of birds exposed to WNV
I_B	0	Amount of infectious birds
R_B	0	Amount of recovered (immune) birds
L_M	0	Amount of mosquito larvae
S_M	$N_{M_{min}}$	Amount of susceptible mosquitoes
E_M	0	Amount of mosquitoes exposed to WNV
I_M	0	Amount of infectious mosquitoes

Carrying capacity of mosquito larvae. To estimate the capacity for any model region in Germany, we first studied the literature to find the maximum density in a perfect habitat in Central Europe. We then adjusted this value to the size of the model region and multiplied it by the mean percentage habitat suitability according to Kerkow et al. (2019). To determine the highest possible population density, we considered a study in the Netherlands (Ibañez-Justicia et al., 2018), in which several sample plots were examined in large allotment garden complexes where *Ae. j. japonicus* has been established for several years. Allotment gardens are ideal habitats for *Ae. j. japonicus* due to their rich vegetation structure, irrigation systems and the presence of numerous suitable breeding habitats (rain barrels, flower pots etc.). All possible breeding habitats were counted in the study and the larvae identified. At the time of the highest larval density (September 2015), 242 containers on an area of 6.8 ha contained 4,335 larvae of *Ae. j. japonicus*. This results in 63,750 larvae/ km^2, of which an estimated 31,875 are female, assuming an equal distribution of the sexes. Based on these observations, we have set the maximum carrying capacity $K_{M_{max}}$ to 19,900,000 for our study regions, which cover 625 km ^{2}.

2.3.4. Parameter estimation

The constant parameters in the differential equations are summarised in Table 2. They were each determined on the basis of the results of literature research. See chapter “Constant parameters” in the appendix for further explanations. Temperature and daylength dependent parameters are summarised in table (Table 3). Again, a detailed description of these parameter calculations can be found in the appendix. However, we would like to be more precise about the calculation of the transmission rate ($\beta_B(T)$) at this point.

The transmission rate from an infectious bird to a susceptible mosquito ($\beta_B(T)$) is the product of the bird biting rate, the proportion of bird bites on host birds, and the transmission efficiency p_B. To what extent *Ae. j. japonicus* visit the WNV host bird species compared to other bird species is not specifically known for central Europe. It is likely that bird species whose habitats overlap with those of the mosquitoes will be preferred, and that a high bird species diversity reduces the likelihood of a vector mosquito encountering a host bird. We made model applications with the assumption that specimens of the species *Ae. j. japonicus* do not prefer any bird species for their blood meals. Since in Germany the magpie accounts for about 5.7% of the total bird population (Geodon et al., 2014, p. 59 and p. 397), we integrated that factor in the transmission rates and found that, with this setting, transmission cycles cannot occur in any scenario. Only when at least 50% of the avian blood meals are taken on this host bird, epizootics can be triggered in the warmest region of Germany (R 3). This is why we work with a 75% preference factor for magpies over other bird species in the model applications presented here.

Table 2
Constant parameters.

Term	Description	Value	Reference
m_B	Average mortality rate of magpies	0.001404 d^{-1}	Tatner (1986)
γ_B	Rate infected–infectious magpies	0.333 d^{-1}	de Oya et al. (2018)
ν_B	Portion of magpies dying due to WNV infection	0.43	de Oya et al. (2018)
α_B	Removal rate of magpies due to WNV infection	0.28 d^{-1}	de Oya et al. (2018)
p_M	Transmission efficiency from infectious mosquito to bird	1.0	de Oya et al. (2018), Sardelis and Turell (2001)
p_B	Transmission efficiency from infectious bird to mosquito	0.17	Veronesi et al. (2018)
P	Proportion of *Ae. j. japonicus* blood meals taken on birds	0.18	Schönenberger et al. (2016)

Table 3
Temperature and daylength dependent parameters.

Parameter description	Function
Biting rate	$k(T) = \frac{0.344}{1 + 1.231e^{-0.184T-20}}$
Larva hatching rate	$b_L(T) = 2.325k(T)$
Mosquito hatching rate	$b_M(T) = 0.1b_L(T)$
Larva mortality rate	$m_L(T) = 0.0025T^2 - 0.094T + 1.0257$
Mosquito mortality rate	$m_M(T) = 0.1m_L(T)$
Transmission rate I_M to S_B	$\beta_M(T) = 0.75Pk(T)p_M$
Transmission rate I_B to S_M	$\beta_B(T) = 0.75Pk(T)p_B$
Rate infected-infectious mosquitoes	$\gamma_M(T) = \frac{1}{0.0093T - 0.1352}$ for $T > 15$; else: 0
Fraction active *Ae. j. japonicus*	$\delta_J(D) = 1 - \frac{1}{1 + 40,000e^{1.559(D(d-30)-18.177)}}$
Hatching rate magpies	$b_B(x) = 0.614\frac{(x/\beta)^{\alpha-1}e^{-(x/\beta)}}{\beta\Gamma(\alpha)}$, $x > 0$, $\alpha = 4.43$, $\beta = 7.67$
Transformed Julian calendar day	$x = d - 120$

2.4. Spatial component

2.4.1. Agents

In the spatial component, the mosquitoes are bundled together to form super-agents (super-mosquitoes) which only unite individuals with the same infection status. Super-agents are a common way to speed up the runtime of an ABM with a large number of agents (Parry and Bithell, 2012). One super-mosquito can comprise 10, 100 or 1,000 individuals, depending on the setting. We here present model applications with a super-agent factor of 10. For the visualisation of infectious mosquitoes, the factor should not exceed 100, for the visualisation of all mosquitoes, however, a factor of 1,000 is advisable to keep the computing time at an acceptable level.

The super-mosquitoes are characterised by the study region, the position within the grid (row, column), the stage of infection (either infectious or not infectious) and an energy level (it is not energy in the biological sense but rather a kind of probability of further survival.) In addition, it is recorded whether a super-mosquito tried to leave the region during the entire model run and if so, in which cardinal direction.

Birds are not implemented on an individual level in the model and not exactly located. We assume the vector birds to move widely in comparison to the mosquitoes and being equally present throughout. Interaction between birds and mosquitoes only exists in so far as the mosquitoes visit birds for their blood meals. However, since we assume an equal spatial distribution of the birds, the proportion of infected mosquitoes and birds caused by the infection forces is only numerically calculated and then the infectious mosquitoes are added (as super-mosquitoes) to or removed from the spatial flight simulation.

2.4.2. Flight behaviour

With each simulation step, the super-mosquitoes can move on the grid map with 100 m × 100 m resolution and a size of 625 km^2 (we call it "mosquito world") in any direction within the Moore neighbourhood. The distance they travel has some stochasticity, but it is controlled by a flight motivation resulting from the habitat suitability of the current location, and additionally by the main wind direction in the study region when the habitat suitability at the current location is poor. If the habitat is well suited, a super-mosquito will most likely remain there or not fly far. In cells with medium habitat quality, it mostly stays there, but sometimes flies further to meet its needs. In an unsuitable habitat, it is more likely to fly long distances than in habitats with medium suitability. This enables the super-mosquito to leave this location more quickly. Every super-mosquito constantly loses energy every day to a small extent, and a potentially large amount due to long-distance flights. The energy can be recharged during stays in good habitats. If a certain threshold value is exceeded, they die. The energy equation was set up in such a way that observations on population trends in the regions in Germany, where *Ae. j. japonicus* occurs, can be reproduced. The motivations and resulting distances are defined based on the following considerations:

Flight motivations. Active dispersal rates of female mosquitoes are generally dependent on the density and distribution of their preferred blood hosts, the availability of breeding habitats, terrain characteristics, and weather (Petrić et al., 2014; Verdonschot and Besse-Lototskaya, 2014). Regarding terrain characteristics, vegetation and land use play a particularly important role. They can represent natural barriers, ecological corridors and stepping stones for dispersal. Landscapes that support the spread of *Ae. j. japonicus* are mosaics of smaller deciduous forests (less than 500 ha), vineyards and areas with private houses and gardens. Barriers, however, are e.g. large forest areas and intensively cultivated fields (Sáringer-Kenyeres et al., 2020; Seidel et al., 2016; Tannich, 2015).

Based on the insights described above, we have introduced a flight motivation in the flight simulator which is landscape dependent. We differentiate between low, medium and high motivations, which are assigned to the mosquitoes when they are in cells with values ≥ 0.8 to 1.0, ≥ 0.3 to 0.8 and 0 to < 0.3. According to the model of Kerkow et al. (2019) whose output we use as a basis for the mosquito worlds, the category with the highest habitat quality (1.0 to ≥ 0.8) includes discontinuous urban fabrics, green urban areas, cemeteries, gardens, zoos, and deciduous forests. The middle one (0.8 to ≥ 0.3) covers most notably mixed forests, woodland–shrub transition zones, fruit and berry plantations, and the last one (< 0.3 to 0) mainly landscapes with an open character such as farmland, pastures and airports, but also continuous urban fabrics and coniferous forests.

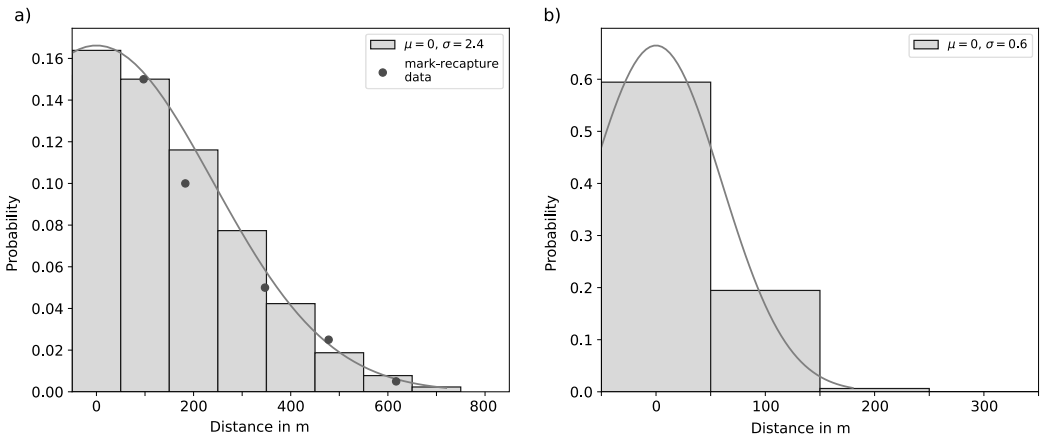

Fig. 4. Distribution curves used to generate random flight distances for (a) moderately motivated and (b) low motivated super-mosquitoes.

Flight distances. For *Ae. j. japonicus* we are not aware of any published results of mark-recapture experiments that would help to estimate the flight distances in certain landscapes and under certain weather conditions. There is evidence that individuals in a perfect habitat do not fly long distances and hardly spread out, which may explain the findings that larger contiguous forest areas sometimes act more as barriers than as corridors. For a location in Belgium (a second-hand tire company with a neighbouring small woodland) no evidence of dispersion could be found even after 6 years, although there are suitable stepping stones, a settlement in direct connection as well as further woodlands and tree rows at distances of only a few hundred metres linear distance (Egizi et al., 2016). Also, species of the genus *Aedes* and especially the urban-domestic, container-breeding species are known to be rather weak flyers (Verdonschot and Besse-Lototskaya, 2014) and no behaviour like that of long-distance fliers was documented for *Ae. j. japonicus*, i.e. ascending high into the air immediately after adult emergence, facilitating far wind drifts (Service, 1980).

An approximate indication of flight distances is given by a documentation of the spread of *Ae. j. japonicus* in West Germany (North Rhine-Westphalia) (Kampen et al., 2016). There, an average dispersal of about 10 km to 20 km per year was recorded between 2012 and 2015, with some exceptions of up to 50 km. As it is known that *Ae. j. japonicus* also spreads passively to a large extent, especially along roads (Egizi et al., 2016), we suggest that the exceptional dispersal rates exceeding 2 km/year are due to this cause (as stated before, the flight simulator only takes into account self-motion of mosquitoes and no passive dispersal). Assuming that the annual main activity and thus the dispersal period is 200 days/year (from mid-March to mid-October), the maximum flight distances would range from 500 m to 1 km/day.

Evaluations of mark-recapture experiments of various mosquito species show that most individuals remain at the site and the probability of recapture decreases with increasing distance (Verdonschot and Besse-Lototskaya, 2014). To the summarised data on *Ae. albopictus*, which is also described as a weak flyer like *Ae. j. japonicus* and which has similar habitat requirements, we have fitted a normal distribution (Fig. 4a) to generate probabilities for the flight ranges of *Ae. j. japonicus* super-agents with medium flight motivation (we did not consider a fat-tail distribution as often used in dispersal modelling of e.g. pollen (Nathan et al., 2012) since we do not model passive motions that would allow for increased long-distance dispersal). The data was divided by 100 before the fitting to convert the metres to map units. The distribution has the mean value at zero and a standard deviation (σ) of 2.4. For super-mosquitoes with low flight motivation, we have reduced the standard deviation of the fitted normal distribution to 0.6 so that they rarely fly further than 100 m or 200 m and the probability of staying in the cell is relatively high (Fig. 4b).

To determine the flight direction and next location of a low and medium motivated super-mosquito on the grid map, its flight range is randomly divided into two segments: Westward/Eastward and Northward/Southward. The direction taken in each case is determined by the algebraic sign of the randomly generated flight distance and by means of another random generator.

We assume that the mosquitoes fly longer distances in unsuitable habitats as they are not able to satisfy all their needs (availability of breeding habitats, host animals or shelter provided by vegetation). Therefore, we implemented a random generator for the super-mosquitoes in these habitats, which generates equally distributed flight distances between 0 map units and 3 to 4 map units (depending on wind conditions) for Westward/Eastward and the Northward/Southward movements, respectfully. This results in a maximum flight distance of 424 m (3 map units) to 566 m (4 map units) per day, when the (super-) mosquito flies the direct route in a diagonal direction of the Moore neighborhood.

Various studies in wind tunnels and in the field show that mosquitoes are more likely to fly upwind than downwind (Kennedy, 1940; Midega et al., 2012; Endo and Eltahir, 2018). This is probably due to the appetising flights in which they follow smells that are transported by the wind (Verdonschot and Besse-Lototskaya, 2014). At wind speeds of 3 km/h and above, however, many species stop flying and seek shelter on the ground or in the vegetation (Service, 1980).

As stated above, the poor mosquito habitats are mainly open landscapes offering limited protection, so we assume that the influence of the wind is particularly noticeable in these. Using data from the surrounding weather stations of the study regions, we analysed the main wind directions and found that for each region, movement in a westerly and southerly direction would be more likely (Fig. 5). Hence, we let the super-mosquitoes fly up to 400 m towards west and south and up to 300 m towards north or east. This results in a 1.3 times higher probability of a super-mosquito flying in the direction with the stronger wind conditions.

2.4.3. Boundary effects

We have implemented two options for the area boundaries of the study regions. In "open" mode, the super-mosquitoes can leave the region and the loss is compensated by hatchings (see Section 2.4.5) of new super-mosquitoes with the same infection status. This mode merely prevents a potential mass accumulation at the edge of the study region. In "closed" mode, the super-mosquitoes cannot leave the region. An emigration attempt is registered and the cardinal point is saved on the first time. However, the flight is not executed and the super-mosquito remains in its cell. The distribution pattern hardly differs between the applications of both options (we could not observe any mass accumulation of super-mosquitoes at the borders in closed mode). However, the calculation time is significantly longer in the open mode, so we will only apply the closed mode in this work.

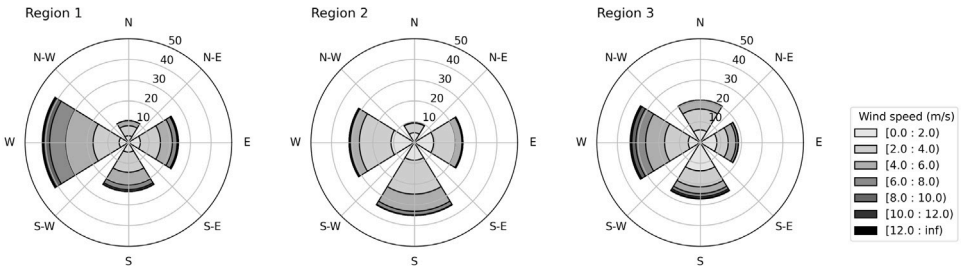

Fig. 5. Wind roses showing the multi-annual distribution averages of wind speeds and directions for the 3 study sites within the period 2011–2019.

2.4.4. Energy

The super-mosquitoes in the flight simulator have an energy level that causes them to die during long stays in unsuitable habitats or after covering large distances. This makes large areas with unfavourable conditions to dispersion barriers. It is known that long distance flights are highly energy consuming for mosquitoes (Verdonschot and Besse-Lototskaya, 2014), but we have no information about the distance covered by *Ae. j. japonicus* under certain habitat conditions. We thus adapted the energy control in a way that a significant reduction of the population can occur in region 1, but the population remains stable in regions 2 and 3. This is consistent with observations made in systematic monitorings (Koban et al., 2019; Kampen et al., 2016).

For the energy level of a super-mosquito, which can take on values between 1 and 100, we use the following balance equation:

$$\frac{dE}{dt} = \delta_{\text{prev}} E - \delta_{\text{const}} - \delta_{\text{flight}} F + bQ \tag{12}$$

where δ_{prev} is the inverse time unit, E is the energy on the previous time unit, δ_{const} is a constant energy loss per time unit, δ_{flight} is the energy loss per flight distance and time unit, F is the Euclidian flight distance between the start and destination cells (the cells have a resolution of $100 \times 100\,\text{m}^2$, so the distance is given in hectometres), b is a boosting factor per time unit, and Q is the quality value of the new cell (the quality values are between 0 and 1 and we handle them equivalent to energy units per time unit). For the simulations, we set $\delta_{\text{prev}} = 1$ per time unit, $\delta_{\text{const}} = 4\,\text{EU}$ (energy units) per time unit, $\delta_{\text{flight}} = 8\,\text{EU}$ per time unit and flight distance, and $b = 50\,\text{EU}$ per time unit.

2.4.5. Control of all super-mosquitoes

To apply certain processes (hatchings, deaths) to all super-mosquitoes in the simulation, we have drawn up two lists at a higher hierarchical level in the programme. They contain the infectious and non-infectious super-mosquitoes with all their characteristics. On this level, we also count the number of super-mosquitoes that have tried to leave the region and whether it was the first time.

Hatching. The hatching function is used for 3 different purposes. Firstly, to locate the super-mosquitoes on the first day of simulation (spatial initialisation), secondly, when the SEIR model calculates an increase in mosquitoes compared to the previous day, and thirdly, when super-mosquitoes have emigrated in open model mode and this loss is to be compensated.

By hatchings, the super-mosquitoes appear at random locations in the study area, but preferably in patches with good habitat qualities. The larvae are not represented in the spatial component for runtime reasons, but the mosquitoes hatch in the larval breeding sites, which are implemented based on the following considerations: The greater the habitat suitability, the more breeding sites should be available since the presence of these was one of the main considerations when preparing the habitat suitability map (Kerkow et al., 2019). The breeding sites of *Ae. j. japonicus* are water-filled natural or artificial containers such as flower dishes, cemetery vases, wells or tree holes. They are often not permanently present and filled with water, so their location should be habitat-related but also have a stochastic component. Furthermore, breeding habitats may be located outside but close to actual main habitats.

To achieve this, we have created copies from the habitat maps and reduced its spatial resolution to 500 m × 500 m (in the following, we refer to 100 m × 100 m units on the map as *cells* and larger areas measuring 500 m × 500 m as *patches*). The values of all individual habitat qualities within each 25 ha patch were summed up and again scaled to values between 0 and 1 for each study region. The super-mosquitoes first hatch on the low-resolution map. A weighted random generator ensures higher hatching rates with increasingly better habitat suitability. The super-mosquitoes are then transferred back to the original map with 100 m × 100 m resolution. The allocation within each 25 ha patch is random. All newly hatched super-mosquitoes start with the maximum energy level of 100.

Deaths. If the temporal model component reduces the number of mosquitoes compared to the previous day (this happens almost every day in autumn) and if, as a result, the number of mosquitoes is lower than in the spatial component, then the corresponding number of super mosquitoes in the respective infection stage is also removed from the spatial component. The selection is random. Super-mosquitoes that have died due to a loss of energy are already included in the comparison.

2.4.6. Observation

For each time step, the number of larvae, the number of mosquitoes and birds in their respective infection states, and the number of super-mosquitoes that have emigrated (open mode) or tried to emigrate at least once (closed mode) in the respective directions (see Chap. 2.4.3) can be displayed. For this purpose, the data are stored during the simulation. Furthermore, the spatial distribution of all super-mosquitoes and the infected super-mosquitoes is stored in arrays. Using these, we display (i) the movements of the mosquitoes during the entire simulation period in a video and (ii) the distribution of the super-mosquitoes on the day with the highest infections in a single map.

3. Results

As the composite model is not validated, does not include all major WNV hosts and vectors, and as the rate of blood meals on the host birds is unknown (it can vary considerably from region to region), the calculated amplitude of WNV case numbers in birds and the infection rate in mosquitoes is not yet reliable. For the sake of completeness, we have presented these results in the appendix.

The results of the spatial distributions of the *Ae. j. japonicus* populations in late summer (at the time when most infectious mosquitoes are present) show that the super-mosquitoes accumulate strongly in cells with very good habitat qualities (values from 0.8 to 1) (Fig. 6). The majority of these cells contain deciduous forests and human settlements in all 3 study regions (see Fig. 2).

In region 1, very poor and very good habitats are particularly strongly separated from each other (Fig. 1a). This enables to assess the spatial extent at which a dispersion barrier is effective. The energy and flight distance settings resulted in the super-mosquitoes moving a

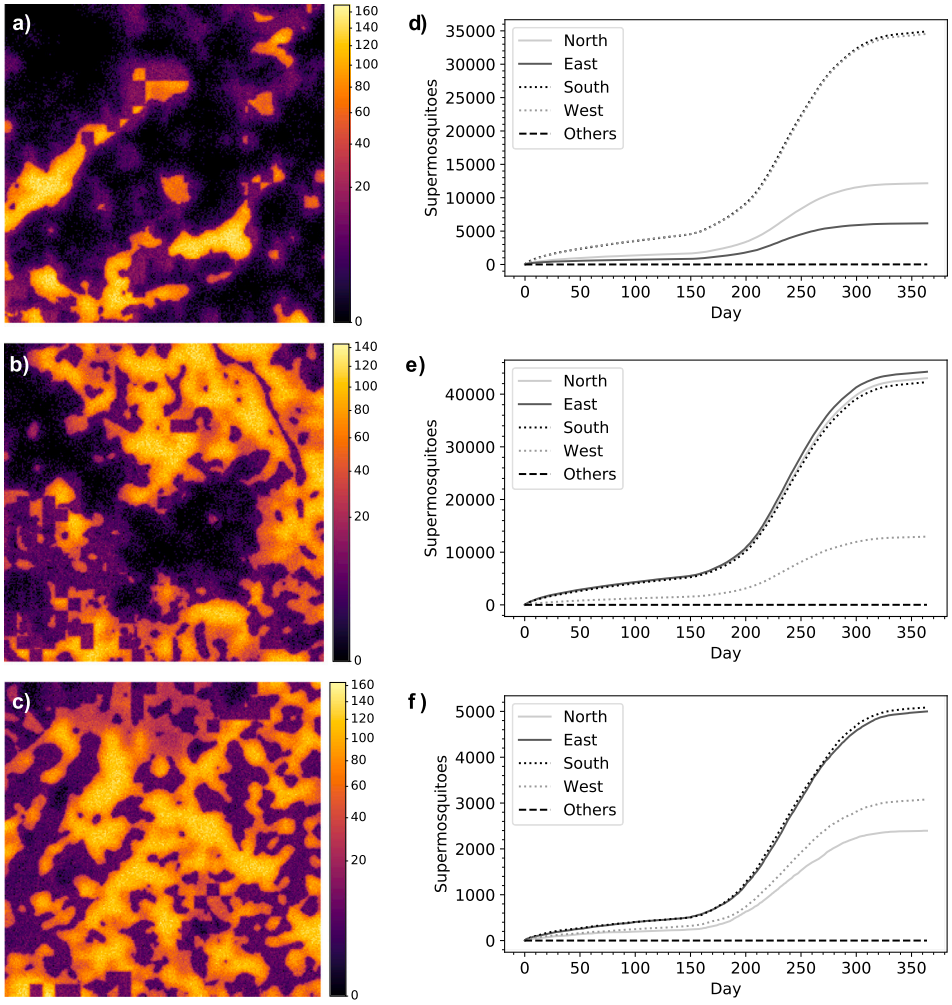

Fig. 6. Left: Distribution of female, non-diapausing super-mosquitoes in all stages of infection at the day with the highest number of infectious mosquitoes in study region 1 (a), 2 (b) and 3 (c); Right: Cumulative number of super-mosquitoes that attempted to emigrate to each of the cardinal points for the first time during the entire simulation period in study region 1 (d), 2 (e) and 3 (f). The term "Others" stands for the options north-east, south-east, south-west and north-west.

maximum of about 2 km away from the very good habitats. Already at a distance of 1 km, the super-mosquito density decreases rapidly. As a result, the area with the poor conditions in the centre was not a strong dispersion barrier, but an area in the north-east of the region remained super-mosquito-free throughout the simulation (Video S1, Fig. 6a). Also in region 2, many super-mosquitoes are able to cross the area with poor habitat characteristics, which extends from the north-west to the centre and is mainly characterised by arable land (video S2, Fig. 6b). Small towns and villages between the crop lands serve as stepping stones (Fig. 2e).

The number of super-mosquitoes being eliminated from the simulation during the entire simulation period due to low energy levels was about 228,700, 53,600 and 134,200 for regions 1, 2 and 3, respectively (Table 4). The reduction in total maximum mosquito population from applications of the linked model in 2018 compared to applications of the SEIR model without spatial extension was 9.82% in Region 1, 1.1% in Region 2, and 0.05% in Region 3 (Table 5). In region 1, repeated use of model applications resulted in a higher risk of infected super-mosquitoes being prematurely removed from the simulation than in the regions 2 and 3. This is due to the large proportion of unfavourable habitats in region 1.

The number of total emigration attempts is almost three times higher in region 3 and almost twice as high in region 2 than in region 1. However, if only the first emigration attempts are considered, the differences are smaller (Table 4, Fig. 6). In region 1, approximately the same number of super-mosquitoes emigrate towards south and west during the entire simulation. On the one hand, these are the main wind directions in all study regions (Fig. 5) and, on the other hand, more areas with high occurrence probabilities have intersections with the borders in the west and south of region 1.

In region 2, about the same number of super-mosquitoes made the first attempt to emigrate towards the north, east and south. Much less good and very good mosquito habitats border the eastern edge of the region, and only a third of the super-mosquitoes tried to leave the region for the first time in this direction. In region 3, there were about twice as many first attempts to emigrate towards the east and south as towards the north or west. Also here, the result is related to the very good mosquito habitats located along the edge of the region and not to the main wind directions.

Runtime. The application of the coupled model to the year 2018 on a machine with an Intel(R) Core(TM) i7-4510U processor with 4 CPU lasts 9 min, 20 min and 28 min for the 3 study regions, respectively, and a super-mosquito factor of 100. Without saving the arrays for each simulation day which serves to create the flight videos, the runtime is reduced by about 3 min. With a super-mosquito factor of 1.000, the runtime can be reduced even more to a maximum of 3 min. However, with a factor of 10, the runtime is 6 h 13 min for region 1, 1 d 1 h 47 min for region 2 and 1 d 6 h 22 min for region 3.

Table 4
Emigration attempts and energy-related deaths of super-mosquitoes (1 super-mosquito refers to 10 individuals) in the application of the linked model for the year 2018.

	First emigration attempts						Total attempts	Energy-related deaths	
	North	East	South	West	Others	Sum		$S_M + E_M$	I_M
Region 1	12,167	6,165	34,922	34,542	14	87,810	111,701,473	228,685	1
Region 2	43,028	44,251	42,274	12,960	11	142,524	217,099,996	53,621	0
Region 3	22,923	49,596	50,841	31,226	7	154,593	321,748,672	134,199	0

Table 5
Comparison of the development of mosquito populations as well as the course of infection measured by the maximum number of infected mosquitoes and birds in model applications with and without spatial coupling.

		SEIR	Coupled model
Region 1	N_M	10,429,570.00	9,405,828.00
Region 1	I_M	89.71	47.77
Region 1	I_B	5.76	4.40
Region 2	N_M	19,046,930.00	18,852,660.00
Region 2	I_M	372.22	362.76
Region 2	I_B	18.42	17.98
Region 3	N_M	26,893,620.00	26,881,040.00
Region 3	I_M	5241.68	5234.14
Region 3	I_B	225.22	224.94

4. Discussion

We introduce the first compartment model for West Nile virus, which also simulates the abundance and movements of a vector mosquito species in a spatial extension and thus helps to estimate where virus hotspots could be located and towards which direction the virus is likely to be carried from a region by active flights of the mosquitoes. The temporal component (SEIR model) is exploratory. This means that the results are not yet validated. The SEIR model was adapted to the conditions in Central Europe and a realistic size of the mosquito population. Originally, the SEIR model was implemented for Minneapolis in the US and validated with the number of detected dead sentinel birds (Laperriere et al., 2011). The flight simulator is implemented on the basis of literature studies and we scaled it in such a way that population development data available for all three study regions could be reproduced.

4.1. Temporal model component

Validation of the results of our exploratory SEIR model applications is not possible because (i) the evidence of WNV-RNA in German wild bird populations is still very low, (ii) it is uncertain whether the Eurasian magpie is or will be a major vector in Central Europe, (iii) there are very likely several bird and mosquito species that act as efficient hosts and vectors, so the model should be extended to deal with this, and (iv) there is still a lack of clarity about multiple factors that influence the vector competence of *Ae. j. japonicus*. This includes in particular the degree of ornitophily and the rate of blood meals on the corresponding host bird species. Furthermore, we coupled the model components in such a way that poor habitat structures negatively affect mosquito populations, thus the spatial model plausibly intervenes in the equations of the original SEIR model.

Other uncertainties include that data on the virus incubation period among vector mosquitoes in relation to temperature is extremely limited and that the function used here is based solely on an experiment with *Cx. tarsalis*. In addition, the results of laboratory experiments on *Ae. j. japonicus* to investigate the dissemination rate and transmission efficiency for WNV are not consistent. While Huber et al. (2014) found resistance to infection in individuals from south-west Germany and could not identify co-infections with other flavi-viruses or the *Wolbachia* bacterium of the mosquitoes which could bias the results, Veronesi et al. (2018) were able to demonstrate dissemination rates of 15.6% for strain NY99 and 18.3 for FIN in Swiss individuals.

Furthermore (v), the carrying capacity of *Ae. j. japonicus* larvae in the study regions is only estimated based on a habitat map derived from a nested modelling approach (Kerkow et al., 2019) and on a study indicating the larval abundance in an ideal habitat. The habitat map, however, was not validated with abundance data but with occurrence data mainly derived from the citizen science project "Mueckenatlas" (Walther and Kampen, 2017). A check of the correlation between abundance data from a systematic monitoring and of the different habitat qualities, as performed for example in the studies of Mushinzimana et al. (2006) and Chaves and Moji (2017), is therefore an important project for the future.

There are additional factors that may play a role in the development of a WNV epizootic that we have not considered to focus on the essential factors and to not excessively modify the evaluated SEIR baseline model. First, the development of the mosquito population in the model is dependent on the carrying capacity of the larvae, temperature-dependent hatching and death rates, and the proportion of non-diapausing mosquitoes as a function of the season. In fact, winter frosts (Reuss et al., 2018) and precipitation (Chianese et al., 2019) also affect population development.

Moreover, there is evidence that some species of mammals and amphibians, e.g. squirrels, rabbits and frogs, are also susceptible to WNV infection and develop high levels of viraemia. This way of transmission, however, is supposed to play only a minor role (Chancey et al., 2015).

The model neglects vertical transmission paths for mosquitoes and horizontal paths for host birds. However, there are indications for vertical (trans-ovarian) transmissions in different species of the *Culex* genus. The transmission efficiency can vary between 10 to 40% (Nelms et al., 2013). It is also assumed that vertically infected mosquitoes facilitate the hibernation of the virus in many regions (Calistri et al., 2010; Ciota, 2017; Dohm et al., 2002; Nelms et al., 2013). However, no published results are yet available indicating vertical transmission of WNV in *Ae. j. japonicus*. Birds can become infected horizontally through consumption of infected birds of prey, feather-picking and oral contact with the faeces of other birds. Horizontal transmission in birds could play a major role. It is suspected to be the reason why birds of prey and feather-pickers, such as crows and hawks, become infected in nature frequently (Komar et al., 2003; Yaremych et al., 2004; Pérez-Ramírez et al., 2014). Scenario analyses to investigate the effects of different trans-ovarian transmission rates in mosquitoes and horizontal transmission rates in birds remain an important future task for disease modellers, but adjustments can easily be made in the SEIR model.

The influence of infections of the birds and mosquitoes with other pathogens is also neglected in our model. However, the susceptibility of host birds may be affected by previous infections with viruses from the group of Japanese encephalitis viruses, which includes the Usutu virus occurring in Germany (Pérez-Ramírez et al., 2014). The vector competence of the mosquitoes as well as population size and sex ratio can also be influenced by cross-infection with the bacterium *Wolbachia pipientis* (Ciota, 2017; Gao et al., 2020).

4.2. Spatial model component

The flight simulator can predict the locations of mosquito hotspots within a region as well as dispersion barriers and stepping stones for

potentially infected mosquitoes of the species *Ae. j. japonicus*. The flight simulations can also be used to assess how efficiently the virus can spread from a region to the respective cardinal points through active flights of the mosquitoes. This is useful after a sudden local introduction of the virus as it was the case in 2018 in some places in Germany. As the model is freely available and based on free software, it can be adapted to new research results and applied to other regions.

As mentioned in chapter 4.1, the model needs to be extended for other vector mosquito species. We have implemented the flight simulator for the Japanese bush mosquito *Ae. j. japonicus*, since there are yet no comparable high-resolution habitat maps for Germany available for other vector species like *Cx. pipiens*, further species of the *Culex agg.*, or *Ae. vexans*.

Although numerous studies provide information on the propagation speed of the invasive Japanese bush mosquito (Damiens et al., 2014; Seidel et al., 2016; Egizi et al., 2016; Kampen et al., 2016; Montarsi et al., 2019), it is not possible to determine the extent of the influence of passive propagation by traffic in any of the observations. Studies suggest that *Ae. j. japonicus* and other invasive species of the genus *Aedes* spread over longer distances by means of transport (Egizi et al., 2016; Eritja et al., 2017). However, in our model we have concentrated on the active spread of the mosquito. One reason for this is that transport-assisted dispersal must involve different control measures than dispersal away from transport routes by the self-motion of mosquitoes. On the other hand, there are already models that estimate long-distance spreads of the virus by birds (Maidana and Yang, 2008, 2009), or a combination of long-distance spread by both, birds and mosquitoes (Liu et al., 2006).

The flight simulator is implemented as an agent-based model. ABMs are computationally intensive and therefore not well suited to deal with large numbers of individuals, such as millions of mosquitoes in our case. However, by bundling several mosquitoes into super-mosquitoes, we were able to bring the run times into an acceptable range of only several minutes with a super-mosquito factor of 1,000. The other side of agent models is that they can be extended in many ways. Thus, additional host bird and vector mosquito species, each with different virus transmission characteristics, could be added in the future resulting in a multi-agent model.

5. Conclusions

We have adapted a WNV compartment (Susceptible–Exposed–Infectious–Removed) model for both a potential host bird and vector mosquito species (*Pica pica* and *Aedes japonicus japonicus*) occurring in Germany and coupled it with a flight simulator for the vector mosquitoes. The flight simulator is an agent-based model built on a habitat map for the mosquito species being invasive in Germany, data on local temperature and wind conditions, and studies on the flight behaviour of this and other mosquito species.

The spatial extension of the SEIR model is the first step in developing a tool that can estimate for a region (i) whether an epizootic can emerge after virus introduction, (ii) how large the vector mosquito population is, and (iii) where vector mosquito hot spots, dispersal corridors, stepping stones and barriers are located. In addition, (iv) the model can calculate the probability of infectious mosquitoes leaving the region in the respective cardinal directions. The model extension is not only a visualisation tool, but also intervenes in the differential equations of the SEIR model. This applies in particular to regions with few suitable habitats, where the potential size of the mosquito population is reduced on a daily basis as a result of long flight distances.

Since many bird and mosquito species are hosts and vectors of West Nile virus, the current version of the model cannot yet reliably determine the extent of an epizootic. In a next step, it must be expanded to include other important bird and mosquito species with their respective life-trait parameters, virus incubation times, transmission rates, and so forth. Moreover, we plan to extend the model further so that the coupled model can run in parallel for many, somewhat smaller patches with presumably different numbers of host birds.

The spatially extended WNV model, implemented in Python 3.7, is freely available under the Creative Commons Attribution - Non Commercial 4.0 (https://github.com/akerkow/bush-mosquito-flight-simulator) and a tool aimed at modellers involved in planning control measures for WNV vector mosquitoes. It is particularly useful for applications in regions where the virus has been recently introduced. For model applications, we recommend selecting the size of the study area to cover the territories of the host birds surrounding the reported WNV cases. Local ornithologists may be consulted to assist with this. It would also be advantageous if blood meal data were available for the relevant mosquito species for the region under study.

CRediT authorship contribution statement

Antje Kerkow: Conception of the study, Conducted the literature research, Designed the model, Analysed and interpreted the model results, Drafted the manuscript. **Ralf Wieland:** Designed the model, Critically revised the manuscript. **Jörn M. Gethmann:** Contributed parasitological and epidemiological expert knowledge, Critically revised the manuscript. **Franz Hölker:** Contributed expert knowledge for the conception of agent based models, Critically revised the manuscript. **Hartmut H.K. Lentz:** Supported the data analyses, Critically revised the manuscript.

Declaration of competing interest

The authors declare that they have no known competing financial interests or personal relationships that could have appeared to influence the work reported in this paper.

Funding

This work was supported by the Federal Ministry of Food and Agriculture, Germany (BMEL, grant no. 2819105315) and the Ministry of Science, Research and Culture of the Federal State of Brandenburg (MWFK), Germany.

Appendix A. Supplementary data

Supplementary material related to this article can be found online at https://doi.org/10.1016/j.ecolmodel.2021.109840.

References

Apperson, C.S., Hassan, H.K., Harrison, B.A., Savage, H.M., Aspen, S.E., Farajollahi, A., Crans, W., Daniels, T.J., Falco, R.C., Benedict, M., Anderson, M., McMillen, L., Unnasch, T.R., 2004. Host feeding patterns of established and potential mosquito vectors of West Nile virus in the eastern United States. Vector-Borne Zoonotic Dis. 4 (1), 71–82. http://dx.doi.org/10.1089/153036604773083013.

Bażanów, B., Jansen van Vuren, P., Szymański, P., Stygar, D., Frącka, A., Twardoń, J., Kozdrowski, R., Pawęska, J.T., 2018. A survey on West Nile and Usutu viruses in horses and birds in Poland. Viruses 10 (2), 87. http://dx.doi.org/10.3390/v10020087.

Bhowmick, S., Gethmann, J., Conraths, F.J., Sokolov, I.M., Lentz, H.H.K., 2020. Locally temperature - driven mathematical model of West Nile virus spread in Germany. J. Theoret. Biol. 488, 110117. http://dx.doi.org/10.1016/j.jtbi.2019.110117.

Brock, T.D., 1981. Calculating solar radiation for ecological studies. Ecol. Model. 14 (1), 1–19. http://dx.doi.org/10.1016/0304-3800(81)90011-9.

Brownstein, J.S., Rosen, H., Purdy, D., Miller, J.R., Merlino, M., Mostashari, F., Fish, D., 2002. Spatial analysis of West Nile virus: Rapid risk assessment of an introduced vector-borne zoonosis. Vector-Borne Zoonotic Dis. 2 (3), 157–164. http://dx.doi.org/10.1089/15303660260613729.

Brugger, K., Rubel, F., 2009. Simulation of climate-change scenarios to explain Usutu-virus dynamics in Austria. Prevent. Vet. Med. 88 (1), 24–31. http://dx.doi.org/10.1016/j.prevetmed.2008.06.023.

Calistri, P., Giovannini, A., Hubalek, Z., Ionescu, A., Monaco, F., Savini, G., Lelli, R., 2010. Epidemiology of West Nile in Europe and in the Mediterranean Basin. Open Virol. J. 4, 29–37. http://dx.doi.org/10.2174/1874357901004010029.

Chancey, C., Grinev, A., Volkova, E., Rios, M., 2015. The global ecology and epidemiology of West Nile virus. BioMed. Res. Int. 2015 (376230), 20. http://dx.doi.org/10.1155/2015/376230.

Chaves, L.F., Moji, K., 2017. Density dependence, landscape, and weather impacts on aquatic *Aedes japonicus japonicus* (Diptera: Culicidae) abundance along an urban altitudinal gradient. J. Med. Entomol. 55 (2), 329–341. http://dx.doi.org/10.1093/jme/tjx200.

Chianese, A., Stelitano, D., Astorri, R., Serretiello, E., Della Rocca, M.T., Melardo, C., Vitiello, M., Galdiero, M., Franci, G., 2019. West Nile virus: An overview of current information. Transl. Med. Rep. 3 (8145), 21. http://dx.doi.org/10.4081/tmr.8145.

Ciota, A.T., 2017. West Nile virus and its vectors. Curr. Opin. Insect Sci. 22, 28–36. http://dx.doi.org/10.1016/j.cois.2017.05.002.

Cooke, W.H., Grala, K., Wallis, R.C., 2006. Avian GIS models signal human risk for West Nile virus in Mississippi. Int. J. Health Geogr. 5 (1), 36. http://dx.doi.org/10.1186/1476-072X-5-36.

Damiens, D., Ayrinhac, A., Bortel, W.V., Versteirt, V., Dekoninck, W., Hance, T., 2014. Invasive process and repeated cross-sectional surveys of the mosquito *Aedes japonicus japonicus* establishment in Belgium. PLOS ONE 9 (4), e89358. http://dx.doi.org/10.1371/journal.pone.0089358.

de Almeida, S.J., Martins Ferreira, R.P., Eiras, A.E., Obermayr, R.P., Geier, M., 2010. Multi-agent modeling and simulation of an *Aedes aegypti* mosquito population. Environ. Model. Softw. 25 (12), 1490–1507. http://dx.doi.org/10.1016/j.envsoft.2010.04.021.

de Oya, N.J., Camacho, M.-C., Blázquez, A.-B., Lima-Barbero, J.-F., Saiz, J.-C., Höfle, U., Escribano-Romero, E., 2018. High susceptibility of magpie (*Pica pica*) to experimental infection with lineage 1 and 2 West Nile virus. PLOS Negl. Trop. Dis. 12 (4), e0006394. http://dx.doi.org/10.1371/journal.pntd.0006394.

Diuk-Wasser, M.A., Brown, H.E., Andreadis, T.G., Fish, D., 2006. Modeling the spatial distribution of mosquito vectors for West Nile virus in Connecticut, USA. Vector-Borne Zoonotic Dis. 6 (3), 283–295. http://dx.doi.org/10.1089/vbz.2006.6.283.

Dohm, D.J., Sardelis, M.R., Turell, M.J., 2002. Experimental vertical transmission of West Nile virus by *Culex pipiens* (Diptera: Culicidae). J. Med. Entomol. 39 (4), 640–644. http://dx.doi.org/10.1603/0022-2585-39.4.640.

Durand, B., Tran, A., Balança, G., Chevalier, V., 2017. Geographic variations of the bird-borne structural risk of West Nile virus circulation in Europe. PLOS ONE 12 (10), e0185962. http://dx.doi.org/10.1371/journal.pone.0185962.

Egizi, A., Kiser, J., Abadam, C., Fonseca, D.M., 2016. The Hitchhiker's guide to becoming invasive: Exotic mosquitoes spread across a US state by human transport not autonomous flight. Mol. Ecol. 25 (13), 3033–3047. http://dx.doi.org/10.1111/mec.13653.

Endo, N., Eltahir, E.A.B., 2018. Modelling and observing the role of wind in *Anopheles* population dynamics around a reservoir. Malar. J. 17 (1), 48. http://dx.doi.org/10.1186/s12936-018-2197-5.

Eritja, R., Palmer, J.R.B., Roiz, D., Sanpera-Calbet, I., Bartumeus, F., 2017. Direct evidence of adult *Aedes albopictus* dispersal by car. Sci. Rep. 7 (1), 1–15. http://dx.doi.org/10.1038/s41598-017-12652-5.

Filippelli, G.M., Freeman, J.L., Gibson, J., Jay, S., Moreno-Madriñán, M.J., Ogashawara, I., Rosenthal, F.S., Wang, Y., Wells, E., 2020. Climate change impacts on human health at an actionable scale: a state-level assessment of Indiana, USA. Clim. Change 163, 1985–2004. http://dx.doi.org/10.1007/s10584-020-02710-9.

Forsythe, W.C., Rykiel, E.J., Stahl, R.S., Wu, H.-i., Schoolfield, R.M., 1995. A model comparison for daylength as a function of latitude and day of year. Ecol. Model. 80 (1), 87–95. http://dx.doi.org/10.1016/0304-3800(94)00034-F.

Früh, L., Kampen, H., Kerkow, A., Schaub, G.A., Walther, D., Wieland, R., 2018. Modelling the potential distribution of an invasive mosquito species: comparative evaluation of four machine learning methods and their combinations. Ecol. Model. 388, 136–144. http://dx.doi.org/10.1016/j.ecolmodel.2018.08.011.

Gao, H., Cui, C., Wang, L., Jacobs-Lorena, M., Wang, S., 2020. Mosquito microbiota and implications for disease control. Trends Parasitol. 36 (2), 98–111. http://dx.doi.org/10.1016/j.pt.2019.12.001.

Geodon, K., Grüneberg, C., Mitschke, A., Sudfeldt, C., Eikhorst, W., Fischer, S., Flade, M., Frick, S., Geiersberger, I., Koop, B., Kramer, M., Krüger, T., Roth, N., Ryslavy, T., Stübing, S., Sudmann, S.R., Steffens, R., Vökler, F., Witt, K., 2014. Atlas of German Breeding Birds, first ed. Stiftung Vogelmonitoring Deutschland and Dachverband Deutscher Avifaunisten, Münster.

Harrigan, R.J., Thomassen, H.A., Buermann, W., Smith, T.B., 2014. A continental risk assessment of West Nile virus under climate change. Global Change Biol. 20 (8), 2417–2425. http://dx.doi.org/10.1111/gcb.12534.

Holicki, C.M., Ziegler, U., Răileanu, C., Kampen, H., Werner, D., Schulz, J., Silaghi, C., Groschup, M.H., Vasić, A., 2020. West Nile virus lineage 2 vector competence of indigenous *Culex* and *Aedes* mosquitoes from Germany at temperate climate conditions. Viruses 12 (5), 561. http://dx.doi.org/10.3390/v12050561.

Hubálek, Z., Kosina, M., Rudolf, I., Mendel, J., Straková, P., Tomešek, M., 2018. Mortality of goshawks (*Accipiter gentilis*) due to West Nile virus lineage 2. Vector-Borne Zoonotic Dis. 18 (11), 624–627. http://dx.doi.org/10.1089/vbz.2018.2289.

Hubálek, Z., Tomešek, M., Kosina, M., Šikutová, S., Straková, P., Rudolf, I., 2019. West Nile virus outbreak in captive and wild raptors, Czech Republic, 2018. Zoonoses Public Health 66 (8), 978–981. http://dx.doi.org/10.1111/zph.12638.

Huber, K., Jansen, S., Leggewie, M., Badusche, M., Schmidt-Chanasit, J., Becker, N., Tannich, E., Becker, S.C., 2014. *Aedes japonicus japonicus* (Diptera: Culicidae) from Germany have vector competence for Japan encephalitis virus but are refractory to infection with West Nile virus. Parasitol. Res. 113 (9), 3195–3199. http://dx.doi.org/10.1007/s00436-014-3983-9.

Ibañez-Justicia, A., Teekema, S., den Hartog, W., Jacobs, F., Dik, M., Stroo, A., 2018. The effectiveness of Asian bush mosquito (*Aedes japonicus japonicus*) control actions in colonised peri-urban areas in the Netherlands. J. Med. Entomol. 55 (3), 673–680. http://dx.doi.org/10.1093/jme/tjy002.

Jourdain, E., Toussaint, Y., Leblond, A., Bicout, D., Sabatier, P., Gauthier-Clerc, M., 2007. Bird species potentially involved in introduction, amplification, and spread of West Nile virus in a Mediterranean wetland, the Camargue (Southern France). Vector-Borne Zoonotic Dis. 7 (1), 15–33. http://dx.doi.org/10.1089/vbz.2006.0543.

Kampen, H., Holicki, C.M., Ziegler, U., Groschup, M.H., Tews, B.A., Werner, D., 2020. West Nile virus mosquito vectors (Diptera: Culicidae) in Germany. Viruses 12 (5), 493. http://dx.doi.org/10.3390/v12050493.

Kampen, H., Kuhlisch, C., Fröhlich, A., Scheuch, D.E., Walther, D., 2016. Occurrence and spread of the invasive Asian bush mosquito *Aedes japonicus japonicus* (Diptera: Culicidae) in West and North Germany since detection in 2012 and 2013, respectively. PLOS ONE 11 (12), e0167948. http://dx.doi.org/10.1371/journal.pone.0167948.

Kampen, H., Schuhbauer, A., Walther, D., 2017. Emerging mosquito species in Germany - a synopsis after 6 years of mosquito monitoring (2011–2016). Parasitol. Res. 116 (12), 3253–3263. http://dx.doi.org/10.1007/s00436-017-5619-3.

Kennedy, J.S., 1940. The visual responses of flying mosquitoes. Proc. Zoolog. Soc. Lond. A109 (4), 221–242. http://dx.doi.org/10.1111/j.1096-3642.1940.tb00831.x.

Kerkow, A., Wieland, R., Früh, L., Hölker, F., Jeschke, J.M., Werner, D., Kampen, H., 2020. Can data from native mosquitoes support determining invasive species habitats? Modelling the climatic niche of *Aedes japonicus japonicus* (Diptera, Culicidae) in Germany. Parasitol. Res. 119 (1), 31–42. http://dx.doi.org/10.1007/s00436-019-06513-5.

Kerkow, A., Wieland, R., Koban, M.B., Hölker, F., Jeschke, J.M., Werner, D., Kampen, H., 2019. What makes the Asian bush mosquito *Aedes japonicus japonicus* feel comfortable in Germany? A fuzzy modelling approach. Parasites Vectors 12 (1), 106. http://dx.doi.org/10.1186/s13071-019-3368-0.

Knighton, J., Dapkey, T., Cruz, J., 2014. Random walk modeling of adult *Leuctra ferruginea* (stonefly) dispersal. Ecol. Inform. 19, 1–9. http://dx.doi.org/10.1016/j.ecoinf.2013.11.001.

Koban, M.B., Kampen, H., Scheuch, D.E., Frueh, L., Kuhlisch, C., Janssen, N., Steidle, J.L.M., Schaub, G.A., Werner, D., 2019. The Asian bush mosquito *Aedes japonicus japonicus* (Diptera: Culicidae) in Europe, 17 years after its first detection, with a focus on monitoring methods. Parasit. Vectors 12 (1), 109. http://dx.doi.org/10.1186/s13071-019-3349-3.

Komar, N., Langevin, S., Hinten, S., Nemeth, N., Edwards, E., Hettler, D., Davis, B., Bowen, R., Bunning, M., 2003. Experimental infection of North American birds with the New York 1999 strain of West Nile virus. Emerg. Infect. Diseases 9 (3), 311–322. http://dx.doi.org/10.3201/eid0903.020628.

la Puente, J.M.-d., Ferraguti, M., Ruiz, S., Roiz, D., Llorente, F., Pérez-Ramírez, E., Jiménez-Clavero, M.A., Soriguer, R., Figuerola, J., 2018. Mosquito community influences West Nile virus seroprevalence in wild birds: Implications for the risk of spillover into human populations. Sci. Rep. 8 (1), 2599. http://dx.doi.org/10.1038/s41598-018-20825-z.

Laperriere, V., Brugger, K., Rubel, F., 2011. Simulation of the seasonal cycles of bird, equine and human West Nile virus cases. Prevent. Vet. Med. 98 (2), 99–110. http://dx.doi.org/10.1016/j.prevetmed.2010.10.013.

Leggewie, M., Badusche, M., Rudolf, M., Jansen, S., Börstler, J., Krumkamp, R., Huber, K., Krüger, A., Schmidt-Chanasit, J., Tannich, E., Becker, S.C., 2016. *Culex pipiens* and *Culex torrentium* populations from Central Europe are susceptible to West Nile virus infection. One Health 2, 88–94. http://dx.doi.org/10.1016/j.onehlt.2016.04.001.

Linke, S., Niedrig, M., Kaiser, A., Ellerbrok, H., Müller, K., Müller, T., Conraths, F.J., Mühle, R.-U., Schmidt, D., Köppen, U., Bairlein, F., Berthold, P., Pauli, G., 2007. Serologic evidence of West Nile virus infections in wild birds captured in Germany. Am. J. Trop. Med. Hyg. 77 (2), 358–364. http://dx.doi.org/10.4269/ajtmh.2007.77.358.

Liu, R., Shuai, J., Wu, J., Zhu, H., Liu, R., Shuai, J., Wu, J., Zhu, H., 2006. Modeling spatial spread of West Nile virus and impact of directional dispersal of birds. Math. Biosci. Eng. 3 (1), 145–160. http://dx.doi.org/10.3934/mbe.2006.3.145.

Maidana, N.A., Yang, H.M., 2008. Assessing the spatial propagation of West Nile virus. Biophy. Rev. Lett. 03 (01n02), 227–239. http://dx.doi.org/10.1142/S179304800800071X.

Maidana, N.A., Yang, H.M., 2009. Spatial spreading of West Nile virus described by traveling waves. J. Theoret. Biol. 258 (3), 403–417. http://dx.doi.org/10.1016/j.jtbi.2008.12.032, Special Issue: Mathematics in Biointeractions.

Manore, C.A., Hickmann, K.S., Hyman, J.M., Foppa, I.M., Davis, J.K., Wesson, D.M., Mores, C.N., 2015. A network-patch methodology for adapting agent-based models for directly transmitted disease to mosquito-borne disease. J. Biol. Dyn. 9 (1), 52–72. http://dx.doi.org/10.1080/17513758.2015.1005698.

Marini, G., Rosà, R., Pugliese, A., Rizzoli, A., Rizzo, C., Russo, F., Montarsi, F., Capelli, G., 2018. West Nile virus transmission and human infection risk in Veneto (Italy): A modelling analysis. Sci. Rep. 8 (1), 14005. http://dx.doi.org/10.1038/s41598-018-32401-6.

Midega, J.T., Smith, D.L., Olotu, A., Mwangangi, J.M., Nzovu, J.G., Wambua, J., Nyangweso, G., Mbogo, C.M., Christophides, G.K., Marsh, K., Bejon, P., 2012. Wind direction and proximity to larval sites determines malaria risk in Kilifi district in Kenya. Nature Commun. 3 (1), 674. http://dx.doi.org/10.1038/ncomms1672.

Molaei, G., Farajollahi, A., Scott, J.J., Gaugler, R., Andreadis, T.G., 2009. Human bloodfeeding by the recently introduced mosquito, *Aedes japonicus japonicus*, and public health implications. J. Am. Mosq. Control Assoc 25 (2), 210–214. http://dx.doi.org/10.2987/09-0012.1.

Montarsi, F., Martini, S., Michelutti, A., Da Rold, G., Mazzucato, M., Qualizza, D., Di Gennaro, D., Di Fant, M., Dal Pont, M., Palei, M., Capelli, G., 2019. The invasive mosquito *Aedes japonicus japonicus* is spreading in northeastern Italy. Parasites Vectors 12 (1), 120. http://dx.doi.org/10.1186/s13071-019-3387-x.

Mushinzimana, E., Munga, S., Minakawa, N., Li, L., Feng, C.-c., Bian, L., Kitron, U., Schmidt, C., Beck, L., Zhou, G., Githeko, A.K., Yan, G., 2006. Landscape determinants and remote sensing of anopheline mosquito larval habitats in the western Kenya highlands. Malar. J. 5 (1), 13. http://dx.doi.org/10.1186/1475-2875-5-13.

Napp, S., Montalvo, T., Piñol-Baena, C., Gómez-Martín, M.B., Nicolás-Francisco, O., Soler, M., Busquets, N., 2019. Usefulness of Eurasian magpies (*Pica pica*) for West Nile virus surveillance in non-endemic and endemic situations. Viruses 11 (8), http://dx.doi.org/10.3390/v11080716.

Nathan, R., Klein, E., Robledo-Arnuncio, J.J., Revilla, E., 2012. Dispersal kernels: review. In: Dispersal Ecology and Evolution. Oxford University Press, Oxford, http://dx.doi.org/10.1093/acprof:oso/9780199608898.003.0015.

Nelms, B.M., Fechter-Leggett, E., Carroll, B.D., Macedo, P., Kluh, S., Reisen, W.K., 2013. Experimental and natural vertical transmission of West Nile virus by California *Culex* (Diptera: Culicidae) mosquitoes. J. Med. Entomol. 50 (2), 371–378. http://dx.doi.org/10.1603/me12264.

Neupert, D., 2020. Neue Infektionen in mehreren Bundesländern: West-Nil-Virus wieder auf dem Vormarsch. https://www.infranken.de/ratgeber/gesundheit/west-nil-virus-neue-infektionen-in-deutschland-muecken-verbreiten-virus-art-3610051.

Pape, W.J., Winters, A.M., Moore, C.G., Lozano-Fuentes, S., Eisen, L., Eisen, R.J., 2008. Predictive spatial models for risk of West Nile virus exposure in eastern and western Colorado. Am. J. Trop. Med. Hyg. 79 (4), 581–590. http://dx.doi.org/10.4269/ajtmh.2008.79.581.

Parry, H.R., Bithell, M., 2012. Large scale agent-based modelling: A review and guidelines for model scaling. In: Heppenstall, A.J., Crooks, A.T., See, L.M., Batty, M. (Eds.), Agent-Based Models of Geographical Systems. Springer Netherlands, pp. 271–308. http://dx.doi.org/10.1007/978-90-481-8927-4_14.

Parry, H.R., Evans, A.J., Morgan, D., 2006. Aphid population response to agricultural landscape change: A spatially explicit, individual-based model. Ecol. Model. 199 (4), 451–463. http://dx.doi.org/10.1016/j.ecolmodel.2006.01.006, Pattern and Processes of Dynamic Mosaic Landscapes – Modelling, Simulation, and Implications.

Pérez-Ramírez, E., Llorente, F., Jiménez-Clavero, M., 2014. Experimental infections of wild birds with West Nile virus. Viruses 6 (2), 752–781. http://dx.doi.org/10.3390/v6020752.

Petrić, D., Bellini, R., Scholte, E.-J., Rakotoarivony, L.M., Schaffner, F., 2014. Monitoring population and environmental parameters of invasive mosquito species in Europe. Parasites Vectors 7 (1), 187. http://dx.doi.org/10.1186/1756-3305-7-187.

Pietsch, C., Michalski, D., Münch, J., Petros, S., Bergs, S., Trawinski, H., Lübbert, C., Liebert, U.G., 2020. Autochthonous West Nile virus infection outbreak in humans, Leipzig, Germany, August to September 2020. Eurosurveillance 25 (46), 2001786. http://dx.doi.org/10.2807/1560-7917.ES.2020.25.46.2001786.

Reuss, F., Wieser, A., Niamir, A., Bálint, M., Kuch, U., Pfenninger, M., Müller, R., 2018. Thermal experiments with the Asian bush mosquito (*Aedes japonicus japonicus*) (Diptera: Culicidae) and implications for its distribution in Germany. Parasites Vectors 11 (1), 81. http://dx.doi.org/10.1186/s13071-018-2659-1.

Rubel, F., Brugger, K., Hantel, M., Chvala-Mannsberger, S., Bakonyi, T., Weissenböck, H., Nowotny, N., 2008. Explaining Usutu virus dynamics in Austria: Model development and calibration. Prevent. Vet. Med. 85 (3–4), 166–186. http://dx.doi.org/10.1016/j.prevetmed.2008.01.006.

Sardelis, M.R., Turell, M.J., 2001. *Ochlerotatus j. japonicus* in Frederick County Maryland: Discovery, distribution, and vector competence for West Nile virus. J. Am. Mosq. Control Assoc. 17 (2), 137–141.

Sáringer-Kenyeres, M., Bauer, N., Kenyeres, Z., 2020. Active dispersion, habitat requirements and human biting behaviour of the invasive mosquito *Aedes japonicus japonicus* (Theobald, 1901) in Hungary. Parasitol. Res. 119 (2), 403–410. http://dx.doi.org/10.1007/s00436-019-06582-6.

Schaffner, F., Kaufmann, C., Hegglin, D., Mathis, A., 2009. The invasive mosquito *Aedes japonicus* in Central Europe. Med. Vet. Entomol. 23 (4), 448–451. http://dx.doi.org/10.1111/j.1365-2915.2009.00825.x.

Schönenberger, A.C., Wagner, S., Tuten, H.C., Schaffner, F., Torgerson, P., Furrer, S., Mathis, A., Silaghi, C., 2016. Host preferences in host-seeking and blood-fed mosquitoes in Switzerland. Med. Vet. Entomol. 30 (1), 39–52. http://dx.doi.org/10.1111/mve.12155.

Seidel, B., Nowotny, N., Bakonyi, T., Allerberger, F., Schaffner, F., 2016. Spread of *Aedes japonicus japonicus* (Theobald, 1901) in Austria, 2011–2015, and first records of the subspecies for Hungary, 2012, and the principality of Liechtenstein, 2015. Parasites Vectors 9, 356. http://dx.doi.org/10.1186/s13071-016-1645-8.

Service, M.W., 1980. Effects of wind on the behaviour and distribution of mosquitoes and blackflies. Int. J. Biometeorol. 24 (4), 347–353. http://dx.doi.org/10.1007/BF02250577.

Simpson, J.E., Hurtado, P.J., Medlock, J., Molaei, G., Andreadis, T.G., Galvani, A.P., Diuk-Wasser, M.A., 2012. Vector host-feeding preferences drive transmission of multi-host pathogens: West Nile virus as a model system. Proc. R. Soc. B: Biol. Sci. 279 (1730), 925–933. http://dx.doi.org/10.1098/rspb.2011.1282.

Tannich, E., 2015. Auswirkungen des Klimawandels auf die Verbreitung krankheitsübertragender Tiere: Importwege und Etablierung invasiver Mücken in Deutschland. (09/2015), Bundesministerium für Umwelt, Naturschutz, Bau und Reaktorsicherheit, Dessau-Roßlau, p. 36, http://docplayer.org/52341166-Auswirkungen-des-klimawandels-auf-die-verbreitung-krankheitsuebertragender.html.

Tatner, P., 1986. Survival rates of urban magpies. Ringing Migr. 7 (2), 112–118. http://dx.doi.org/10.1080/03078698.1986.9673887.

Thomas, D.M., Urena, B., 2001. A model describing the evolution of West Nile-like encephalitis in New York City. Math. Comput. Modelling 34 (7), 771–781. http://dx.doi.org/10.1016/S0895-7177(01)00098-X.

Tran, A., L'Ambert, G., Balança, G., Pradier, S., Grosbois, V., Balenghien, T., Baldet, T., Lecollinet, S., Leblond, A., Gaidet-Drapier, N., 2017. An integrative eco-epidemiological analysis of West Nile virus transmission. EcoHealth 14 (3), 474–489. http://dx.doi.org/10.1007/s10393-017-1249-6.

Tran, A., Sudre, B., Paz, S., Rossi, M., Desbrosse, A., Chevalier, V., Semenza, J.C., 2014. Environmental predictors of West Nile fever risk in Europe. Int. J. Health Geogr. 13 (1), 26. http://dx.doi.org/10.1186/1476-072X-13-26.

Turell, M.J., O'Guinn, M.L., Dohm, D.J., Jones, J.W., 2001. Vector competence of North American mosquitoes (Diptera: Culicidae) for West Nile virus. J. Med. Entomol. 38 (2), 130–134. http://dx.doi.org/10.1603/0022-2585-38.2.130.

Verdonschot, P.F., Besse-Lototskaya, A.A., 2014. Flight distance of mosquitoes (Culicidae): A metadata analysis to support the management of barrier zones around rewetted and newly constructed wetlands. Limnol. - Ecol. Manag. Inland Waters 45, 69–79. http://dx.doi.org/10.1016/j.limno.2013.11.002.

Veronesi, E., Paslaru, A., Silaghi, C., Tobler, K., Glavinic, U., Torgerson, P., Mathis, A., 2018. Experimental evaluation of infection, dissemination, and transmission rates for two West Nile virus strains in European *Aedes japonicus* under a fluctuating temperature regime. Parasitol. Res. 117 (6), 1925–1932. http://dx.doi.org/10.1007/s00436-018-5886-7.

Wagner, S., Mathis, A., Schönenberger, A.C., Becker, S., Schmidt-Chanasit, J., Silaghi, C., Veronesi, E., 2018. Vector competence of field populations of the mosquito species *Aedes japonicus japonicus* and *Culex pipiens* from Switzerland for two West Nile virus strains: *Ae. japonicus* WNV vector competence. Med. Vet. Entomol. 32 (1), 121–124. http://dx.doi.org/10.1111/mve.12273.

Walther, D., Kampen, H., 2017. The citizen science project "Mueckenatlas" helps monitor the distribution and spread of invasive mosquito species in Germany. J. Med. Entomol. 54 (6), 1790–1794. http://dx.doi.org/10.1093/jme/tjx166.

Werner, D., Kampen, H., 2013. The further spread of *Aedes japonicus japonicus*. Parasitol. Res. 112 (10), 3665–3668. http://dx.doi.org/10.1007/s00436-013-3564-3.

Wieland, R., Kerkow, A., Früh, L., Kampen, H., Walther, D., 2017. Automated feature selection for a machine learning approach toward modeling a mosquito distribution. Ecol. Model. 352, 108–112. http://dx.doi.org/10.1016/j.ecolmodel.2017.02.029.

Wonham, M.J., de-Camino-Beck, T., Lewis, M.A., 2004. An epidemiological model for West Nile virus: Invasion analysis and control applications. Proc. R. Soc. B: Biol. Sci. 271 (1538), 501–507. http://dx.doi.org/10.1098/rspb.2003.2608.

Yaremych, S.A., Warner, R.E., Mankin, P.C., Brawn, J.D., Raim, A., Novak, R., 2004. West Nile virus and high death rate in American crows. Emerg. Infect. Diseases 10 (4), 709–711. http://dx.doi.org/10.3201/eid1004.030499.

Zehender, G., Veo, C., Ebranati, E., Carta, V., Rovida, F., Percivalle, E., Moreno, A., Lelli, D., Calzolari, M., Lavazza, A., Chiapponi, C., Baioni, L., Capelli, G., Ravagnan, S., Da Rold, G., Lavezzo, E., Palù, G., Baldanti, F., Barzon, L., Galli, M., 2017. Reconstructing the recent West Nile virus lineage 2 epidemic in Europe and Italy using discrete and continuous phylogeography. In: Paraskevis, D. (Ed.), PLOS ONE 12 (7), e0179679. http://dx.doi.org/10.1371/journal.pone.0179679.

Ziegler, U., Lühken, R., Keller, M., Cadar, D., van der Grinten, E., Michel, F., Albrecht, K., Eiden, M., Rinder, M., Lachmann, L., Höper, D., Vina-Rodriguez, A., Gaede, W., Pohl, A., Schmidt-Chanasit, J., Groschup, M.H., 2019. West Nile virus epizootic in Germany, 2018. Antiviral Res. 162, 39–43. http://dx.doi.org/10.1016/j.antiviral.2018.12.005.

Ziegler, U., Santos, P.D., Groschup, M.H., Hattendorf, C., Eiden, M., Höper, D., Eisermann, P., Keller, M., Michel, F., Klopfleisch, R., Müller, K., Werner, D., Kampen, H., Beer, M., Frank, C., Lachmann, R., Tews, B.A., Wylezich, C., Rinder, M., Lachmann, L., Grünewald, T., Szentiks, C.A., Sieg, M., Schmidt-Chanasit, J., Cadar, D., Lühken, R., 2020. West Nile virus epidemic in Germany triggered by epizootic emergence, 2019. Viruses 12 (4), 448. http://dx.doi.org/10.3390/v12040448.